Journal Homepage: -www.journalijar.com

INTERNATIONAL JOURNAL OF ADVANCED RESEARCH (IJAR)

Article DOI:10.21474/IJAR01/20528
DOI URL: http://dx.doi.org/10.21474/IJAR01/20528

*RESEARCH ARTICLE*

# ON THE DYNAMICS OF MAGNETIC-FIELD COUPLED HETEROGENEOUS OSCILLATORS: A CASE STUDY WITH CHUAOSCILLATOR AND LC TANK CIRCUIT

**Sk Abdul Kader Faruque[1] and Apurba Kumar Nayek[2]**

1. Department of Physics, Mrinalini Datta Mahavidyapith, Kolkata, 700 051, India.
2. Department of Physics, Dum Dum Motijheel College, Kolkata, 700 074, India.

## *Manuscript Info*

***Manuscript History***
Received: 28 December 2024
Final Accepted: 31 January 2025
Published: February 2025

***Key words:-***
Magnetic Field Coupling, Coupled Hetergenousoscillator, Chua circuit, Chaos control, Bifurcation, Multisim™

## *Abstract*

Recent studies have suggested that inductor-based field coupling can effectively control chaos, with potential applications in neurocomputing and neural networks. This article investigates the dynamics of a Chua oscillator coupled with a periodic LC tank circuit via an inductor, presenting numerical simulation results on phase space dynamics. Results for both double-scroll chaotic Chua circuit and limit-cycle Chua circuit are presented and a similardynamics involving intermittent transition between chaotic and ordered state have been observed. A preliminary analysis based on linear stability theory is presented. The basic properties of the model are discussed, such as fixed-point stability, symmetry and dissipation. Numerical simulations, including bifurcation diagrams, Lyapunov spectra, and phase space plots, revealed that the coupling suppresses chaos at specific strengths and leads to multi-periodicity in the periodic regime. Virtual experiment is performed on SPICE-based NI Multisim™ which corroborates the corresponding dynamics.

*"© 2025 by the Author(s). Published by IJAR under CC BY 4.0. Unrestricted use allowed with credit to the author."*

## Introduction:-

Coupled oscillatory system remained a fascinating topic for scientists and researchers since long and have been studied rigorously due to its fundamental importance and application in physics, engineering, biology and several other fields (Pikovsky and Rosenblum 2015; Pikovsky, Rosenblum, and Kurths 2003; Boccaletti et al. 2002; Mosekilde, Maistrenko, and Postnov 2002; González-Miranda 2004). From the viewpoint of dynamics, oscillatory systems can be broadly classified into three distinct categories: periodic, quasi-periodic, and chaotic. The interaction between two oscillatory systems reveals a wide range of intricate and complex dynamical behaviors. To date the study of coupled chaotic oscillators predominantly addresses the interaction between similar systems. In most of the research, the term inhomogeneity or non-identical only refers to similar systems with mismatch in parameters. However, both natural and man-made systems often consist of different adjacent interacting components, with some designed to operate non-linearly and others functioning deterministically. In these systems, one part follows a set of predictable rules, while another part exhibits sensitivity to initial conditions and complex, unpredictable behaviour. In a recent review by Heltberg et. al., the vast nature of rhythms and oscillations found in biological organisms is elaborated and the resulting dynamics due to the interaction between different types of oscillators is discussed (Heltberg et al. 2021). There exists certain pathological conditions, such as, atrial fibrillation and neurological disorder, such as in some forms of epilepsy, where certain regions of the heart or the brain might function in a

**Corresponding Author:- Apurba Kumar Nayek**
Address:- Department of Physics, Dum Dum Motijheel College, Kolkata, 700 074, India.

regular, deterministic manner, while adjacent or coupled regions exhibit chaotic or unpredictable behaviour (Jalife 2000; Tort et al. 2010). In the field of power-electronics-based power systems, such as wind turbine and photovoltaic, the interaction between a single power electronics device connected to an infinite-large system is investigated in the frame-work of recently developed phase-motion equation, and associated dynamical process related to stability is analysed (He et al. 2019). Although interactions between different types of subsystems are abundant in nature, the exact effects of coupling on such heterogeneous systems remain largely understudied. To address the problem of interacting heterogeneous oscillators, mutually coupled quasi-periodic generator and chaotic Rössler oscillator is considered and various dynamical regimes and bifurcation phenomenon are analysed using numerical technique (Kuznetsov, Sedova, and Stankevich 2023). In an effort to explore the dynamics underlying the interaction between two distinct types of oscillators, this article examines the coupling of a chaotic oscillator with a linear passive LC tank circuit. We selected the well-known Chua oscillator as the chaotic component, which is widely studied and frequently used in nonlinear dynamics research. The Chua oscillator can be easily implemented in an electronic circuit that, depending on the circuit parameters, can exhibit a wide range of complex dynamical behaviors, including periodic, quasi-periodic, and chaotic regimes, as well as the famous double scroll attractor. In this study, we have chosen both the double scroll and limit-cycle cases. On the other hand, an LC tank circuit, consisting of an inductor (L) and a capacitor (C) connected in parallel, exhibits sinusoidal oscillations at the circuit's natural resonant frequency, given by $1/2\pi\sqrt{LC}$, due to the continuous exchange of energy between the inductor's magnetic field and the capacitor's electric field. In an ideal scenario with no energy dissipation, these oscillations would continue indefinitely.

The collective behavior of the entire system depends not only on the nature of the individual subsystems but also on the characteristics of the coupling element. Various researchers have investigated chaotic systems interacting via field coupling such as capacitors, inductors, memristors or connected through non-linear elements (Liu et al. 2019; Yao et al. 2020; Chithra and Mohamed 2017). Inductor-based coupling in neuronal activity and neuron-based computing is an emerging concept (C. Wang, Tang, and Ma 2019; Iqbal 2021). Neurons communicate through electrical impulses, and the flow of ions across membranes generates magnetic fields. In principle, inductors could be used to influence these magnetic fields, potentially modulating neuronal activity (H. Wang et al. 2021; Lv et al. 2016). Coexistence of bifurcations and multiple firing patterns in neurons is explained with threshold electromagnetic induction, as well as an asymmetry in the electrical synaptic coupling between two neuronal oscillators, modelled through 2D Hindmarsh-Rose neuron (Njitacke et al. 2020). Inductors can also enhance signal transmission within neuron-based computing systems by reducing energy loss and increasing the speed of signal propagation leading to faster and more efficient neural networks (Kuwahara et al. 2024; Yao et al. 2019). Considering all these developments, the current study employs an inductor as the coupling element.

With this broader objective, the remainder of the article is organized as follows: Sec. **Circuit description and Model Equation** presents the construction of the coupled system and derives the model equation in dimensionless form. Sec. **Elementary dynamical analysis** provides the mathematical formulation of the problem statement. Fixed points, symmetry, dissipativeness and possibility of attractor is established. A rigorous numerical analysis is performed, and the results are detailed in Sec. **Numerical Results**. The phase space dynamics are discussed in terms of the bifurcation diagram, Lyapunov spectrum, and projection of phase space trajectories. Finally, Sec. **Summary and Outlook** summarizes the study and provides an outlook.

**Circuit description and Model Equation**

The chaotic system, considered here is the well known Chua circuit containing an LC oscillator connected to a piecewise linear element, namely, Chua's diode through an RC circuit (Matsumoto, Chua, and Komuro 1985; Madan 1993). The Chua diode can be designed using OPAMP and simple off-the-self resistors following the design procedure as found in (Kennedy 1992). The chaotic Chua oscillator and the periodic LC oscillator system are coupled bidirectionally using a variable inductor $\tilde{L}$. The circuit diagram of the coupled system is shown in **Fig 1(a)**. The Chua oscillator consists of the inductor $L$; capacitors, $C_L$ and $C_1$; resistor $R$, and the Chua diode **NR**. The variable resistor $R$ can be set to values that correspond to the desired behaviour of the Chua oscillator. Inductor $L'$ and capacitor $C'_L$ in parallel forms the periodic LC tank circuit. To maintain identical circuit response, we have taken $L = L'$ and $C_L = C'_L$. The variable inductor $\tilde{L}$ forms the bidirectional coupling between the two systems. A DC voltage source $V$ is connected in parallel to the LC tank circuit through a switch $S$. The voltage source provides initial energy to the passive LC circuit setting it in the oscillating mode. The governing equations for voltage and current can be obtained using Kirchoff's law. $(v_1, v_2, i_L)$ is the set of circuit variables corresponding to the chaotic sub-part and $(v'_2, i'_L)$ is that of the periodic part; where the voltages across the capacitors $C_1$, $C_L$ and $C'_L$ are $v_1$, $v_2$ and $v'_2$, respectively; and

the current through the inductor $L$ and $L'$ are $i_L$ and $i'_L$; $i_N$ is the current through **NR** and can be expressed as a function of voltage $v_1$ as $f(v_1)$, given by $f(v) = G_b v + 0.5(G_a - G_b)(|v + B_p| - |v - B_p|)$, where the parameters, $G_a$ and $G_b$ are the slopes of the inner and outer part of the characteristic curve (shown in **Fig 1(b)**) respectively and $\pm B_p$ represent the break points. The two systems are coupled through the circuit variable $i_L$.

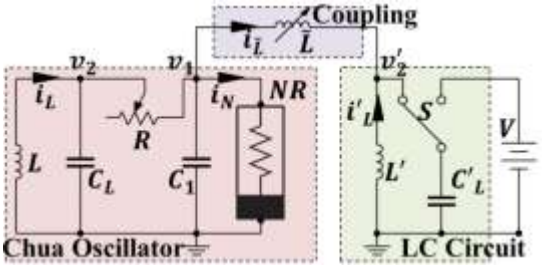


(a) The circuit diagram of the coupled system

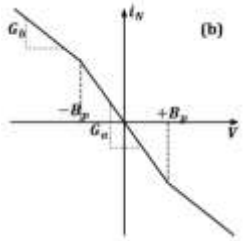


(b) v-i characteristic of the Chua diode, **NR**

**Fig 1.:-** (a) The circuit diagram of showing different parts of the coupled system; (b) The $i$-$v$ characteristics showing piece-wise non-linearity, $i_N$ represents the current through the diode and $v$ is the input voltage, $i_N$ is expressed as function of $v$ ($f(v)$ described in the text).

The governing equations for all the variables can be written using a set of six autonomous $1^{st}$ order ordinary differential equations, which can be reduced to dimensionless form by applying following scaled transformation of variables: $x = v_1/B_p,\ y = v_2/B_p,\ y' = v'_2/B_p,\ z = i_L b_p/R,\ z' = i'_L b_p/R,\ \omega = i_L b_p/R,\ \tau \to t/RC_L$. With this the model equation in dimensionless form is obtained as (in the following $\dot{x}$ and so, refers to derivative with respect to dimensionless time $\tau$)

$$\dot{x} = \alpha(y - x - f(x) - \omega) \quad (1a)$$
$$\dot{y} = x - y + z \quad (1b)$$
$$\dot{z} = -\beta y \quad (1c)$$
$$\dot{y}' = z' + \omega \quad (1d)$$
$$\dot{z}' = -\beta y' \quad (1e)$$
$$\dot{\omega} = \gamma(x - y') \quad (1f)$$

The term $f(x)$ in Eq. (1a) is represented in rescaled form as $f(x) = bx + 0.5(a - b)[|x + 1| - |x - 1|]$ where $a = G_a R$ and $b = G_b R$. The model parameters can be obtained from circuit parameters as: $\alpha = C_L/C_1,\ \beta = R^2 C_L/L,\ \gamma = R^2 C'_L/\tilde{L}$. In the current study, the parameter values set at $a = -1.296$, $b = -0.738$, $\alpha = 10$, $\beta = 18$, which corresponds to the double scroll chaotic regime for the uncoupled oscillator. The parameter $\gamma$ determines the coupling strength which increases with decreasing value of the coupling inductor $\tilde{L}$.

**Elementary dynamical analysis**

**Fixed point analysis**

To start with the dynamical analysis we first review the fixed points (FP) of the coupled system. The fixed points of a $n$-dimensional continous time system of differential equations, given by $\dot{\boldsymbol{X}} = f(\boldsymbol{X})$, where $\boldsymbol{X} \in \mathbb{R}^n$ can be given by solving the set of non-linear equation $f(\boldsymbol{X}) = 0$. As in the case of original Chua oscillator, due to the piecewise non-linearity, the whole phase space can be divided into a set of three distinct regions separated by the hyper-planes $x = -1$ and $x = 1$. We may indicate the regions as $D_{-1}: x \le -1$, $D_0: -1 \le x \le 1$ and $D_1: x \ge 1$. The piece-wise linear function, $f(x)$ can be written in the three regions as follows.

$$f(x) = \begin{cases} bx - (a - b) & if \quad x \le -1 \\ ax & if \quad |x| \le 1 \\ bx + (a - b) & if \quad x \ge 1 \end{cases} \quad (2)$$

It is to be noted that Eq. (1) is linear separately in each of the three regions. The Chua oscillator has three distinct fixed points one each in the three regions, given by $E_1 = (\kappa, 0, -\kappa) \in D_1$, $E_0 = (0,0,0) \in D_0$ and $E_{-1} = (-\kappa, 0, \kappa) \in D_{-1}$, where $\kappa$ is defined as $\kappa = (b - a)/(1 + b)$. On the other hand the periodic LC oscillator has one unique stable fixed point at $(y' = 0, z' = 0)$. If we consider the coupled equations (1) as a single system the dynamics can be described in a six-dimensional space. The fixed points are obtained as

$$\begin{aligned} E_1^c &= (0,0,0,0,-a+b,a-b) \in D_1 \\ E_0^c &= (0,0,0,0,0,0,0) \in D_0 \\ E_{-1}^c &= (0,0,0,0,a-b,-a+b) \in D_{-1} \end{aligned} \quad (3)$$

In the above, the superscript $^c$ represents the fixed points for the coupled state. Now, a careful insight in to the expression of the FPs asserts that the nature of the FPs remain almost same except the center of rotation change phase plane. The linear stability of the fixed points can be determined by the $6 \times 6$ Jacobian matrix of the system given by

$$J = \begin{pmatrix} -\alpha\left(1+\frac{df}{dx}\right) & \alpha & 0 & 0 & 0 & -\alpha \\ 1 & -1 & 1 & 0 & 0 & 0 \\ 0 & -\beta & 0 & 0 & 0 & 0 \\ 0 & 0 & 0 & 0 & 1 & 1 \\ 0 & 0 & 0 & -\beta & 0 & 0 \\ \gamma & 0 & 0 & -\gamma & 0 & 0 \end{pmatrix} \quad (4)$$

It can be shown, by computing characteristic equation $|J - \lambda I| = 0$, where $I$ is a $6 \times 6$ unit matrix, that all the eigenvalues of the Jacobian does not have non-negative real parts, that is the FPs are not stable. Hence, we can expect that the coupled system exhibit orbit or chaotic attractor.

**Symmetry and Dissipation**

The system shows symmetry under inversion similar to original Chua Oscillator. Thus, the system behaviour remain invariant under the transformation$\boldsymbol{X} \to -\boldsymbol{X}$, where $\boldsymbol{X}$ denotes the set of state vectors$\boldsymbol{X} = [x, y, z, y', z', w]^T$. The dissipativeness of the system can be asserted by calculating vector field divergence given by $\Lambda = \sum \frac{\partial \dot{x}_i}{\partial x_i}$ where $x_i \in \boldsymbol{X}$, which is simply given by the trace of the Jacobian matrix $(tr(J))$.

$$\Lambda = \alpha\left(1+\frac{df}{dx}\right) - 1 \leq 0$$

Each volume enclosing the system trajectory contracts to zero exponentially at a rate of $\Lambda$ as time $t$ approaches infinity.

Eq. 1 can be written in terms of the Jacobian matrix, $J$, as follows

$$\dot{\boldsymbol{X}} = \begin{cases} J(\boldsymbol{X} \pm \boldsymbol{k}) & if \quad \boldsymbol{X} \in D_{\pm 1} \\ J\boldsymbol{X} & if \quad \boldsymbol{X} \in D_0 \end{cases} \quad (5)$$

where $\boldsymbol{X} = [x, y, z, y', z', w]^T$ and $\boldsymbol{k} = [\kappa, 0,0,0,0,0]^T$, with $\kappa$ as defined above. Hence, we obtain a linear equation separated by the planes $x = 1$ and $x = -1$. The linear equations can be solved by computing the eigenvalues and eigenvectors of the Jacobian matrix, yielding results similar to those observed in the original Chua oscillator, such as the double scroll, periodic and multi-periodic limit cycles, chaotic single scrolls, and other complex behaviors. However, due to the presence of the field coupling term $\gamma$, and depending on the initial conditions, various types of dynamics may emerge, which we will explore numerically in the next section.

## Numerical Results:-

To further investigate the system's dynamics, numerical integration of the ODEs defined by Eq. 1 is performed. The dynamics are explored using various tools such as bifurcation diagrams, Lyapunov spectra, and phase space plots. All numerical calculations and visualizations are carried out using Python and relevant packages, including NumPy, SciPy, and Matplotlib. The parameters are fixed at the values specified in Sec.**Circuit description and Model Equation**, and for each calculation, sufficient initial iterations are discarded as transients to ensure a steady-state solution. The coupling parameter $\gamma$ is varied within the range of 0.03 to 0.16, corresponding to a practically achievable coupling inductor $(\tilde{L})$ range of 2 to 10 H. For experimental validation, the circuit is also implemented in the SPICE-based NI Multisim simulator.

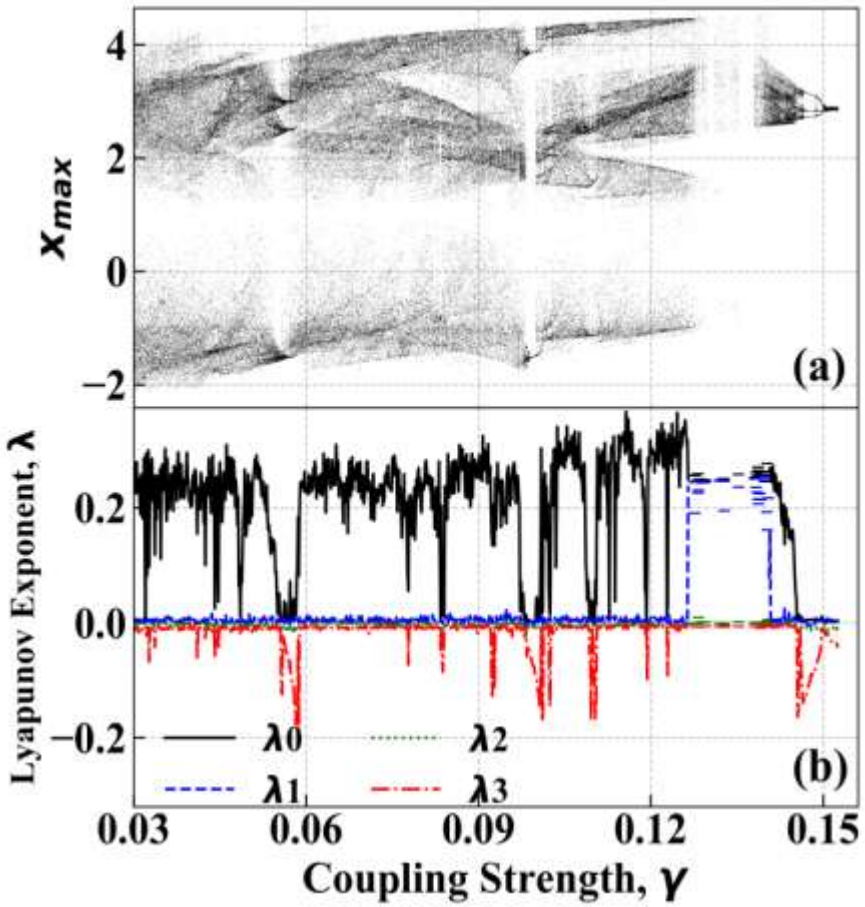


**Fig2:-** Bifurcation diagram and Lyapunov spectrum with $\alpha$ set at 10, corresponding to double scroll attractor (a) Bifurcation diagram of the maximum value of variable $x$ with varying coupling strength, $\gamma$, (b) $1^{st}$ four maximum Lyapunov exponent.

We begin by examining the bifurcation diagram (shown in **Fig2**) to analyze the dynamics of the coupled system. Here, $\alpha$ is set to value 10, which corresponds to double scroll chaotic attractor for the uncoupled oscillator. The bifurcation diagram is generated by varying $\gamma$ across 10000 discrete steps. The integration is performed with fixed initial conditions. Specifically, the initial values for the state variables of the Chua oscillator, i.e. $x$, $y$ and $z$ are fixed at values near the origin $(0,\ 0.1,\ 0.1)$ and the state variables of the LC oscillator $(y',\ z')$ are set at small values of $(0,\ 0.1)$. In practice, this can be achieved by energizing the LC circuit with a DC voltage of 100 mV, which is then removed at $t = 0$ using the switch $S$. The bifurcation diagram is plotted by taking the local maxima of the time series of state variable $x$. The bifurcation diagram provides a clear depiction of the system's dynamics. It can be observed that the system exhibits chaotic dynamics for most values of the coupling constant $\gamma$. However, chaos is suppressed at certain selective values. Period-3 and period-2 limit cycles are observed at $\gamma = 0.05667$ and $\gamma = 0.0989 \sim 0.0999$. In between these values, there are several narrow ranges of $\gamma$, where period-$n$ limit cycle and quasi-periodic behaviour can be observed. As $\gamma$ further increases upto 0.128, the system remains chaotic except for certain values of $\gamma$. Within the range $\gamma = 0.128 \sim 0.140$, instabilities leading to the divergence of trajectories can be observed. This occurs because, in numerical model three segment non-linearity is considered, whereas the practical circuit features a 5-segmented one due to the positive slope of the Chua diode at larger voltage values. It is already demonstrated that when a five segment nonlinearity is taken into account, double scroll attractor coexists with stable external limit cycle (Fortuna, Frasca, and Xibilia 2009). The same is reconfirmed in circuit simulation. As the $\gamma$ value is further increased, the system dynamics goes through a transition from chaotic to periodic oscillation via quasi periodic and period-3 route. Beyond $\gamma = 0.152$, the system becomes unstable. In circuit simulation, further decreasing the value of the coupling inductor $\tilde{L}$ results in the voltages $v_1$, $v_2$ and $v'_2$ oscillating with an amplitude that reaches the saturation voltage of the OPAMPs. This behaviour is observed as a limit cycle on the oscilloscope traces when $v_1$ and $v_2$ are

displayed on the horizontal and vertical channels of the oscilloscope, respectively. The observations from the bifurcation diagram are further complemented by numerical estimation of the spectrum of Lyapunov exponents. The Lyapunov exponents for the continuous-time differential equation are calculated by following the algorithm described in (Wolf et al. 1985). The orthonormalisation of the unit tangent vector is carried out by $\boldsymbol{QR}$ decomposition method after every time evolution of $\tau = 0.1$. The diagonal elements of the $\boldsymbol{R}$ matrix gives the evolution rate, which is then stored and an appropriate mean of 5000 time steps, after removing sufficient transient, is taken to compute the Lyapunov spectrum (Lu et al. 2005). The $1^{st}$ four maximum Lyapunov spectrum of the 6-dimensional system is shown in FIG. 1(b). The chaotic Chua oscillator contributes the positive Lyapunov exponent, while the other two being zero and negative. The LC circuit, contributes one zero and one negative Lyapunov exponent. In the chaotic regime, presence of only one positive Lyapunov exponent excludes any possibility of hyperchaos. In the selective periodicity windows, such as within the range $\gamma = 0.05667$ and $\gamma = 0.0989 \sim 0.0999$, the maximum Lyapunov exponent is zero, with two or three more zero lyapunov exponents. This corroborate the observation of bifurcation diagram and confirms the presence of quasi-periodic behaviour with multiple frequencies.

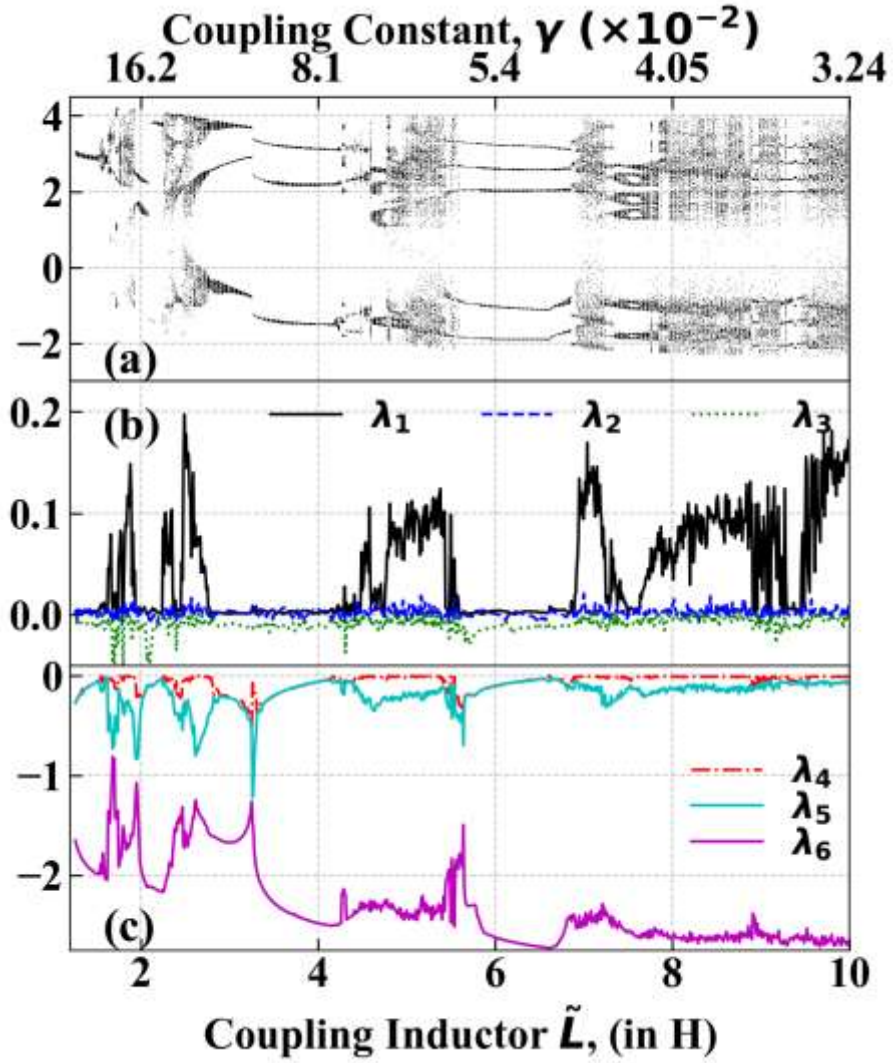


**Fig 3:-** Bifurcation diagram and Lyapunov spectrum with $\alpha$ set at 8.5, corresponding to limit cycle (a) Bifurcation diagram of the maximum value of drive variable $x$ with varying coupling strength, $\gamma$, (b) and (c) Full Lyapunov spectrum.

Similar dynamics can be observed while the Chua oscillator is set to limit cycle mode by setting $\alpha = 8.5$. The corresponding bifurcation diagram and full Lyapunov spectrum is shown in **Fig**3(a) and **Fig 3**(b) - (c), respectively. However, in this case, the periodic regimes are obtained for a larger range of coupling strength, $\gamma$.

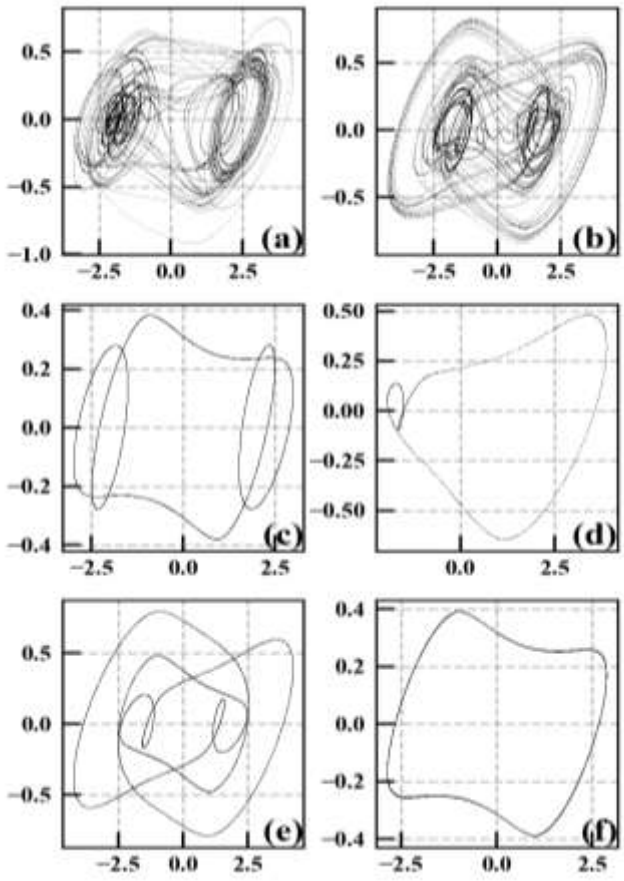


**Fig 4:-** Phase space plot in $x$-$y$ plane showing the dynamics of the Chua oscillator for different values of $\gamma$ in both chaotic ((a) $\gamma = 0.035$ and (b) $\gamma = 0.1021$) and periodic regime ((c) $\gamma = 0.0566$, (d) $\gamma = 0.0995$, (e) $\gamma = 0.1101$, (f) $\gamma = 0.152$).

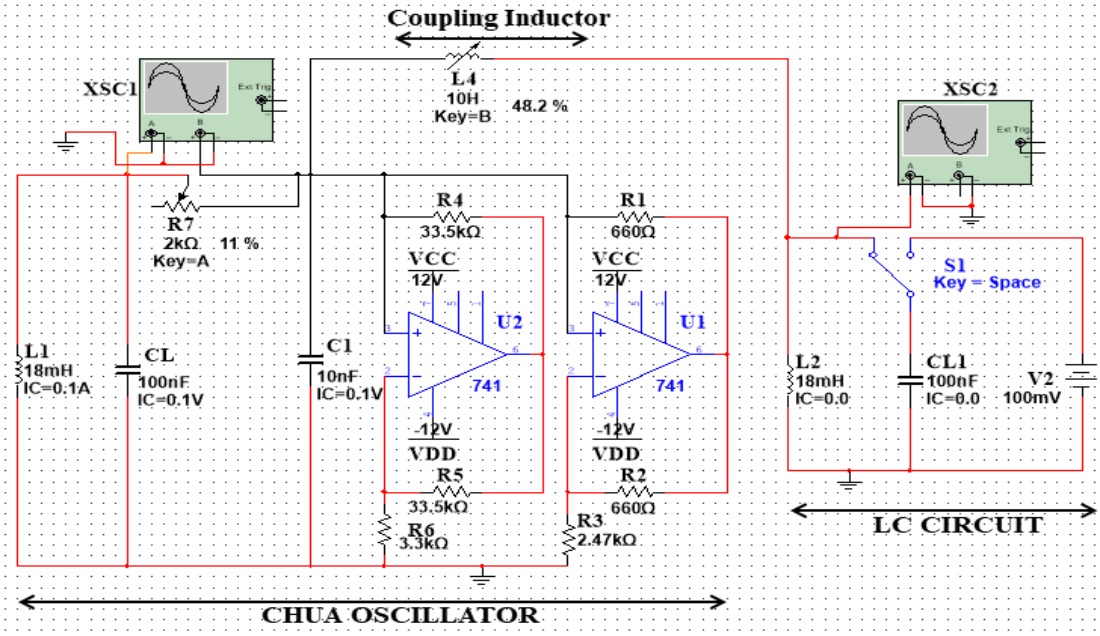


**Fig 5:-** Multisim implementation of the coupled system.

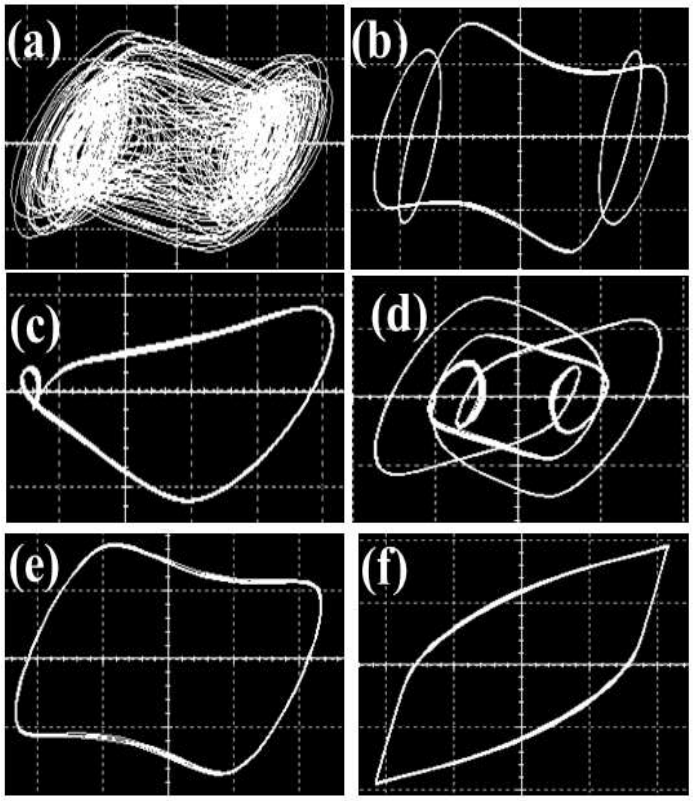


**Fig 6:-** Oscilloscope traces: (a) $\tilde{L} = 9.2$ H, Horizontal axis = 500 mV/div., Vertical axis = 1 V/div.; (b) $\tilde{L} = 5.2$ H, Horizontal axis = 200 mV/div., Vertical axis = 1 V/div.; (c) $\tilde{L} = 3.2$ H, Horizontal axis = 500 mV/div., Vertical axis = 1 V/div.; (d) $\tilde{L} = 2.9$ H, Horizontal axis = 500 mV/div., Vertical axis = 2 V/div.; (e) $\tilde{L} = 2.1$ H, Horizontal axis = 200 mV/div., Vertical axis = 1 V/div.; (f) $\tilde{L} = 1.9$ H, Horizontal axis = 5 V/div., Vertical axis = 5 V/div.

Some of the phase portraits (in the x-y plane) illustrating the dynamics of the coupled oscillator are plotted for both chaotic and periodic/quasi-periodic regime in **Fig 4**. These observations align with the bifurcation diagram and the presence of multiple zero Lyapunov exponents in the Lyapunov spectrum. To this end, the Multisim implementation of the coupled system is shown in Fig. 5. The phase portraits are experimentally simulated with oscilloscope for the Chua oscillator, with some of the oscilloscope traces presented in **Fig 6**. To obtain the traces, the voltage, $v_1$ across the capacitor $C_1$ (representing the state vector x) is plotted on the horizontal axis, while the voltage $v_2$ across the capacitor $C_L$ (representing the state vector y′) is plotted on the vertical axis. The oscilloscope trace are in excellent agreement with the numerical illustration of the phase space plots. Notably, **Fig 6**(f) shows the external limit cycle with both horizontal and vertical axes set at 5 V/div.

**Summary and Outlook**

Mutual or bidirectional coupling between heterogeneous systems via inductor is studied. The chaotic and the linear systems are chosen as Chua oscillator and LC tank circuit, respectively. The circuit equations, derived from Kirchof's law are reduced to dimensionless form for numerical analysis. A mathematical formulation of the model equation is provided in terms of Jacobian matrix and decomposed into linear systems separated by hyperplanes. The phase-space dynamics of the coupled system are analyzed using bifurcation diagrams, Lyapunov exponent spectra, and phase-space plots. Interestingly, the coupling enables chaos suppression at specific values of coupling strength. Phase space plots confirm the existence of quasi-periodic regime with multiple frequencies, corroborating the bifurcation analysis and Lyapunov spectrum. The system is implemented on the Multisim platform for experimental validation, showing excellent agreement with the numerical results. The Chua oscillator exhibits a rich variety of dynamics, such as limit cycle, chaotic as well as double scroll attractor while the LC tank circuit represents the simplest passive sinusoidal oscillator. In this article, we utilize an inductor to couple the systems bidirectionally, exploiting magnetic field-based coupling to facilitate communication between two distinct types of oscillators. This approach reveals several interesting attributes, such as chaos suppression at specific coupling coefficients. As part of

future study, it will be interesting to study any synchronisation-like correlation between the two systems, if any. Although recent research in nonlinear dynamics has increasingly focused on synchronization in complex networks, the fundamental studies presented in this paper can deepen our understanding of the synchronization of different kinds of systems. We further believe that the present study of interactions between heterogeneous systems via inductive coupling can be extended to applications in neuro-computing, neuron-based communication systems, and physiological systems.

## Acknowledgement:-

The authors acknowledge Mr. Bikash Sarkar, Dr. Soumini Chowdhury, and colleagues from the Department of Physics at Mrinalini Datta Mahavidyapith for their support and encouragement. Special appreciation is extended to Dr. Pradeepta Guptaroy, Principal at DDMC &Mr. Sumit Mukhopadhyay, Teacher-in-Charge at MDM, for their invaluable support. The authors also sincerely thank Dr. Anees Akber Butt and Mir Tanvir for their constructive comments and suggestions, which significantly improved this manuscript.

## References:-

1. Boccaletti, S., J. Kurths, G. Osipov, D. L. Valladares, and C. S. Zhou. 2002. “The Synchronization of Chaotic Systems.” Physics Reports 366 (1): 1–101. https://doi.org/10.1016/S0370-1573(02)00137-0.
2. Chithra, A., and I. Raja Mohamed. 2017. “Synchronization and Chaotic Communication in Nonlinear Circuits with Nonlinear Coupling.” Journal of Computational Electronics 16 (3): 833–44. https://doi.org/10.1007/s10825-017-1013-8.
3. Fortuna, Luigi, Mattia Frasca, and Maria Gabriella Xibilia. 2009. “Chua’s Circuit Implementations: Yesterday, Today and Tomorrow.” In, 65:23–27. WORLD SCIENTIFIC. https://doi.org/10.1142/7200.
4. González-Miranda, J. M. 2004. Synchronization and Control of Chaos: An Introduction for Scientists and Engineers. Singapore: World Scientific. https://doi.org/10.1142/p352.
5. He, Miaozhuang, Wei He, Jiabing Hu, Xiaoming Yuan, and Meng Zhan. 2019. “Nonlinear Analysis of a Simple Amplitude–Phase Motion Equation for Power-Electronics-Based Power System.” Nonlinear Dynamics 95 (3): 1965–76. https://doi.org/10.1007/s11071-018-4671-6.
6. Heltberg, Mathias L., Sandeep Krishna, Leo P. Kadanoff, and Mogens H. Jensen. 2021. “A Tale of Two Rhythms: Locked Clocks and Chaos in Biology.” Cell Systems 12 (4): 291–303. https://doi.org/10.1016/j.cels.2021.03.003.
7. Iqbal, Muhammad. 2021. “Modeling and Behavioral Analysis of Neurons Under Direction-Dependent Resistive, Inductive and Capacitive Coupling.” Results in Control and Optimization 3: 100016. https://doi.org/https://doi.org/10.1016/j.rico.2021.100016.
8. Jalife, José. 2000. “Rotors and Spiral Waves in Atrial Fibrillation.” Journal of Cardiovascular Electrophysiology 11 (6): 776–84. https://doi.org/10.1111/j.1540-8167.2000.tb00073.x.
9. Kennedy, M P. 1992. “Robust OP Amp Realization of Chua’s Circuit.” Frequenz 46 (3-4): 66–80. https://doi.org/10.1515/FREQ.1992.46.3-4.66.
10. Kuwahara, Takumi, Reon Oshio, Mutsumi Kimura, Renyuan Zhang, and Yasuhiko Nakashima. 2024. “Fusion Synapse by Memristor and Capacitor for Spiking Neuromorphic Systems.” Neurocomputing 593: 127792. https://doi.org/10.1016/j.neucom.2024.127792.
11. Kuznetsov, Alexander P., Yuliya V. Sedova, and Nataliya V. Stankevich. 2023. “Coupled Systems with Quasi-Periodic and Chaotic Dynamics.” Chaos, Solitons & Fractals 169: 113278. https://doi.org/10.1016/j.chaos.2023.113278.
12. Liu, Zhilong, Jun Ma, Ge Zhang, and Yin Zhang. 2019. “Synchronization Control Between Two Chua’s Circuits via Capacitive Coupling.” Applied Mathematics and Computation 360: 94–106. https://doi.org/10.1016/j.amc.2019.05.004.
13. Lu, Jia, Guolai Yang, Hyounkyun Oh, and Albert C. J. Luo. 2005. “Computing Lyapunov Exponents of Continuous Dynamical Systems: Method of Lyapunov Vectors.” Chaos, Solitons and Fractals 23 (5): 1879–92. https://doi.org/10.1016/j.chaos.2004.07.034.
14. Lv, Mi, Chunni Wang, Guodong Ren, Jun Ma, and Xinlin Song. 2016. “Model of Electrical Activity in a Neuron Under Magnetic Flow Effect.” Nonlinear Dynamics 85 (3): 1479–90. https://doi.org/10.1007/s11071-016-2773-6.
15. Madan, Rabinder N. 1993. Chua’s Circuit: A Paradigm for Chaos. WORLD SCIENTIFIC. https://doi.org/10.1142/1997.

16. Matsumoto, Takashi, Leon Chua, and Motomasa Komuro. 1985. “The Double Scroll.” IEEE Transactions on Circuits and Systems 32 (8): 797–818. https://doi.org/10.1109/TCS.1985.1085791.
17. Mosekilde, Erik, Yuri Maistrenko, and Dmitry Postnov. 2002. Chaotic Synchronization: Applications to Living Systems. Vol. 42. WORLD SCIENTIFIC. https://doi.org/10.1142/4845.
18. Njitacke, Zeric Tabekoueng, Isaac Sami Doubla, Sandrine Mabekou, and Jacques Kengne. 2020. “Hidden Electrical Activity of Two Neurons Connected with an Asymmetric Electric Coupling Subject to Electromagnetic Induction: Coexistence of Patterns and Its Analog Implementation.” Chaos, Solitons & Fractals 137: 109785. https://doi.org/10.1016/j.chaos.2020.109785.
19. Pikovsky, Arkady, and Michael Rosenblum. 2015. “Dynamics of globally coupled oscillators: Progress and perspectives.” Chaos: An Interdisciplinary Journal of Nonlinear Science 25 (9): 097616. https://doi.org/10.1063/1.4922971.
20. Pikovsky, Arkady, Michael Rosenblum, and Jürgen Kurths. 2003. Synchronization: A Universal Concept in Nonlinear Sciences. Cambridge, UK: Cambridge University Press. https://doi.org/10.1017/CBO9780511755743.
21. Tort, Adriano B. L., Robert Komorowski, Howard Eichenbaum, and Nancy Kopell. 2010. “Measuring Phase-Amplitude Coupling Between Neuronal Oscillations of Different Frequencies.” Journal of Neurophysiology 104 (2): 1195–1210. https://doi.org/10.1152/jn.00106.2010.
22. Wang, Chunni, Jun Tang, and Jun Ma. 2019. “Minireview on Signal Exchange Between Nonlinear Circuits and Neurons via Field Coupling.” The European Physical Journal Special Topics 228 (10): 1907–24. https://doi.org/10.1140/epjst/e2019-800193-8.
23. Wang, Hao, Jiahui Wang, Guangyi Cai, Yonghong Liu, Yansong Qu, and Tianzhun Wu. 2021. “A Physical Perspective to the Inductive Function of Myelin — a Missing Piece of Neuroscience.” Frontiers in Neural Circuits 14: 1–23. https://doi.org/10.3389/fncir.2020.562005.
24. Wolf, Alan, Jack B. Swift, Harry L. Swinney, and John A. Vastano. 1985. “Determining Lyapunov Exponents from a Time Series.” Physica D: Nonlinear Phenomena 16 (3): 285–317. https://doi.org/10.1016/0167-2789(85)90011-9.
25. Yao, Zhao, Jun Ma, Yuangen Yao, and Chunni Wang. 2019. “Synchronization Realization Between Two Nonlinear Circuits via an Induction Coil Coupling.” Nonlinear Dynamics 96 (1): 205–17. https://doi.org/10.1007/s11071-019-04784-2.
26. Yao, Zhao, Ping Zhou, Ahmed Alsaedi, and Jun Ma. 2020. “Energy Flow-Guided Synchronization Between Chaotic Circuits.” Applied Mathematics and Computation 374: 124998. https://doi.org/10.1016/j.amc.2019.124998.